Presence of potassium-bearing 2:1 phyllosilicates in B horizons of Ferralsols: Consequences for total and exchangeable potassium content

Ary Bruand [a,*], Michel Brossard [b], Pascal Jouquet [c], Adriana Reatto [d], Jérémie Garnier [e], Julia Mancano Quintarelli [f], Éder de Souza Martins [f]

[a] *Institut des Sciences de la Terre d'Orléans (ISTO), UMR7327, UO – CNRS – BRGM, Observatoire des Sciences de l'Univers en région Centre (OSUC), Université d'Orléans, 1A Rue de la Férollerie, 45071 Orléans Cedex 2, France*
[b] *Institut de Recherche pour le Développement (IRD), Eco&Sols, UMR IRD – INRAE – CIRAD – Institut Agro – University of Montpellier, Montpellier, France*
[c] *Institut de Recherche pour le Développement (IRD), Institute of Ecology and Environmental Sciences of Paris (iEES Paris), UMR Sorbonne Université – UPEC – CNRS – IRD – INRAE, Paris, France*
[d] *Empresa Brasileira de Pesquisa Agropecuária (Embrapa), Secretaria de Pesquisa e Desenvolvimento, Parque Estação Biológica-PqEB s/n⁰, Brasília-DF, Brazil*
[e] *Universidade de Brasília, Instituto de Geociências, Campus Darcy Ribeiro, BR-70910970 Brasília-DF, Brazil*
[f] *Empresa Brasileira de Pesquisa Agropecuária (Embrapa Cerrados), Brasília-DF, Brazil*

ABSTRACT

Although Ferralsols result from a deep weathering, small amounts of potassium-bearing 2:1 phyllosilicates were identified their B horizons in many studies but the consequences on total potassium (K) content and K availability remain under discussion. Our objective was to discuss this issue by measuring the total amount of K, as well as the cation exchange capacity (CEC) and the amount of exchangeable K using chemical analyses of bulk samples, combined with backscattered electron scanning images (BESI) and chemical analyses using energy dispersive X-ray spectroscopy (EDS) on cross-sections of undisturbed samples. Our results showed that the total and exchangeable K were related to the presence of elongated particles corresponding to 2:1 phyllosilicates at varying degrees of weathering. These 2:1 phyllosilicates ranged from weathered muscovite to hydroxy-Al interlayered vermiculites (HIV). The quantities of K reserve potentially available over time for plant nutrition ranged from 259 to 5 044 g ha^{-1} m^{-1}. The stock of exchangeable K$^+$ ranged from 86 to 207 kg ha^{-1} m^{-1} when it was higher than the detection limit (18 kg ha^{-1} m^{-1}). It was related to the density of the elongated particles < 2 μm and 2–20 μm in length because their K was more exchangeable than in larger particles. The CEC varied according to the clay content and the kaolinite proportion in the clay fraction. Finally, if the presence of these K-bearing 2:1 phyllosilicates results, as discussed in recent studies, from the upward material transport activity of termites from the saprolite, this raises the question of the consequences of soil cultivation on soil fauna and hence on the reserve of K and its availability for plant nutrition.

1. Introduction

Potassium (K) is a crucial mineral nutrient for plants that needs to be added to cultivated lands to maintain crop production (Andrist-Rangel et al., 2007; Hinsinger et al., 2021; Sardans and Peñulas, 2015). It is present in soils in different forms: (i) in the soil solution, where it is readily available for plant nutrition, (ii) bound to organic compounds and minerals, where it is also easily exchangeable with other cations in the soil solution, or (iii) in the structure of minerals such as micas and alkaline feldspars, as well as the minerals resulting from their weathering (Bell et al., 2021; Chesworth, 2008; Hinsinger et al., 2021; Öborn et al., 2005). Some of the structural K is available for plant nutrition because it is weakly bound to minerals and thus can be easily exchanged with other cations in the soil solution (Hinsinger et al., 2021; Martin and Sparks, 1985). The total K available for plants in soils can be measured by determining the amount of exchangeable K using various methods, such as those using ammonium acetate, Mehlich-1 reagent, cobalt-hexamine trichloride, or cation exchange resin (Agbenin and van Raij, 1999; Boeira et al., 2004; Bortolon et al., 2010; Ciesielski and Sterckeman, 1997; Pansu and Gautheyrou, 2006). However, part of the non-exchangeable K, particularly that located in the inter-layer space of micas, can subsequently contribute to plant nutrition over time as it is

---

gradually released through weathering processes under specific physico-chemical conditions (Bortoluzzi et al., 2008; Moterle et al., 2016; 2019; Firmano et al., 2020; Hinsinger et al., 2021; Meurer and Anghinoni, 1993; Pal et al., 2001; Poss et al., 1991).

In the tropics, Ferralsols are the predominant soil types. They are red and yellow soils characterized by a deep weathering (IUSS Working Group WRB. 2022). Their fine fraction is primarily composed of low-activity clay (kaolinite), and of gibbsite, goethite, and hematite in varying proportions (Pédro, 1968; van Wambeke, 1992). However, despite their very long geochemical evolution, small amounts of weatherable K-bearing minerals have also been identified in Ferralsols (IUSS Working Group WRB. 2022) and in their corresponding soils in other soil classifications such as the American soil taxonomy (Soil Survey Staff, 2022), the Brazilian soil taxonomy (Embrapa, 2006) and the French Soil Referential (AFES, 2008).

In Togolese and Congolese Ferralsols, small quantities of inter-stratified illite–smectite were indeed identified in the clay fraction by using X-ray diffraction (Mujinya et al., 2013; Poss et al., 1991). In Brazil, X-ray diffraction (XRD) also revealed the presence of weatherable K-bearing minerals in Ferralsols along with micas, vermiculite and hydroxy-Al interlayered vermiculites (HIVs) (e.g. Almeida et al., 2021; Bertolazi et al., 2017; Furian et al., 2002; Ker, 1995; Melo et al., 2004; Maquere et al., 2008; Oliviera et al., 2020; Pacheco et al., 2018; Reatto et al., 2010; Rodrigues Netto, 1996; Schaefer et al., 2008; Soares et al., 2005; Volf et al., 2023). Similarly, X-ray diffraction combined with transmission electron microscopy (TEM) and energy dispersive X-ray spectrometry (EDS), showed the presence of weatherable K-bearing minerals identified in the form of illite in Thai Ferralsols (Darunsontaya et al., 2012). Lastly, the chemical composition of K-bearing 2:1 phyllosilicates was evidenced by combining backscattered scanning electron microscopy and EDS in Brazilian Ferralsols (Bruand et al., 2022; Bruand and Reatto, 2022).

The objective of our study was to analyze the variations of total and exchangeable K content in ferralic B horizons, focusing specifically on the presence of K-bearing minerals. Our aim was to minimize the potential contribution of K bound to organic matter, as it has the ability to be exchanged with cations present in the soil solution. To do so, we used the Brazilian ferralic B horizons studied by Reatto et al. (2007, 2008, 2009a; 2009b) under native vegetation in which the organic matter content was particularly low, thus making it possible to prevent the contribution of K which might be linked to it. We analyzed the presence of K-bearing minerals by combining backscattered electron scanning images (BESI) and EDS. Additionally, we measured the total amount of K, as well as the cation exchange capacity and the amount of exchangeable K. By doing so, we were able to discuss the relationship between the amount of total and exchangeable K pools, without considering the contribution of K bound to soil organic matter. The presence of the K-bearing minerals in the ferralic B horizons studied was also discussed in light of recent studies concerning the role of soil fauna in explaining their presence in the horizons when these result from long and intense weathering.

2. Material and methods

2.1. Study sites and soil material

The Ferralsols studied are located in the Brazilian Central Plateau (Reatto et al., 2007, 2008, 2009a; 2009b). The most representative climate of the Brazilian Central Plateau is Megathermic or Humid Tropical (Aw) with the savanna subtype (Nascimento and Novais, 2020). It is characterized by maximum rains in summer and a dry winter (average temperature of the coldest month > 18 °C). In the region studied, the annual rainfall ranges (1981–2010) from 1,500 to 2,000 mm, and the relative humidity of air from 30 % during the dry season to 75 % during the rainy season (Nascimento and Novais, 2020). Ten ferralic B horizons (FB1 to FB10) of Ferralsols (F1 to F10) corresponding to

the Ferralsols L1 to *L*10 studied earlier by Reatto et al. (2007, 2008, 2009a; 2009b) were selected in the Cerrado (Fig. 1). These Ferralsols have an Ustic moisture regime and a Hyperthermic temperature regime (Soil Survey Staff, 2022). They were described as Orthic Ferralsol or Typic Acrustox (F2, F5 and F7), Rhodic Ferralsol or Rhodic Acrustox (F1, F6, F8, F9 and F10), Xanthic Ferralsol or Xanthic Acrustox (F3) or Plinthic Ferralsol or Plinthic Acrustox (F4) according to the IUSS Working Group WRB (2022) and the Soil Survey Staff (2022), respectively. They were all located under native forest vegetation and developed on a large range of parent materials (granulite: F1; sandy metarythmite: F2 and F3; quartzite: F4; clayey metarythmite: F5; metapelite: F6, F7 and F8; metapelite and limestone: F9; limestone: F10) (Table 1). Their ferralic B horizons were collected at a depth ranging from 0.85 m (FB4) to 1.70 m (FB6) and were highly clayey with a clay content ranging from 30 (FB4) to 78 % (FB6) (Table 1). Their kaolinite content ranged from 19.6 (FB1) to 64.5 % (FB9), their gibbsite content from 18.3 (FB9) to 62.5 % (FB4), their hematite content from 0 (FB3 and FB4) to 20.5 % (FB1) and their goethite content from 0 (FB10) to 17.8 % (FB4) (Table 2).

2.2. Soil analyses

The cation exchange capacity and the exchangeable cations were determined after extraction with the cobaltihexamine chloride (Co$(NH_3)_6Cl_3$) method at 50 mmol$^+$ L^{-1} (ISO, 2018; LAS, 2023). It enables the determination of the cation exchange capacity and the exchangeable cations at a pH close to that of the soil (Ciesielski and Sterckeman, 1997). The amount of the exchangeable cations Al^{3+}, Ca^{2+}, Mg^{2+} and K$^+$ was measured using inductively coupled plasma atomic emission spectrometry (ICP-AES), and H$^+$ using titrimetry. The exchangeable cation Na$^+$ was extracted using ammonium acetate and quantified using microwave plasma atomic emission spectrometry (MP-AES) (LAS, 2023). The total contents in Al, Fe, Mg, Ca, K and Na were determined after extraction with fluorohydric and perchloric acids using ICP-AES. The total contents in Si and Ti were determined after extraction with sodium peroxide using ICP-AES (LAS, 2023). The stocks of total K and exchangeable K were computed using the results of the chemical analysis expressed in g per kg of oven dried soil and cmol$_+$ per kg of oven dried soil, respectively. They were expressed in kg per ha by using the value of bulk density (Table 1) and computed for ferralic B horizons 1 m thick.

Undisturbed samples were collected, dried and then embedded in a polyester resin (Bruand et al., 1996). After polymerization and hardening, circular cross sections 2.5 cm in diameter were prepared and carbon coated for examination by scanning electron microscopy (SEM) using backscattered electron scanning images (BESI) (Bruand et al., 1996). Observations at high magnification (×500 to × 5000) were used to identify particles of phyllosilicates in the groundmass of the microgranular aggregates as being elongated particles with an internal sheet structure (Bruand et al., 2022; Bruand and Reatto, 2022). The scanning electron microscope (SEM) used was a Merlin Compact Zeiss microscope (resolution of 0.8 nm at 15 kV and 1.6 nm at 1 kV; voltage ranging from 20 V to 30 kV; probe current ranging from 12 pA to 100 nA). It was equipped with a Gemini I column including a backscattered electron detector (BSD) with five quadrants for acquisition of BES. Observations were performed at 15 kV accelerating voltage and at a working distance of 10 mm.

Chemical analyses were performed using energy dispersive X-ray spectroscopy (EDS) (Goldstein et al., 2018) with a Quantax XFlash6 Bruker detector enabling a resolution of 129 eV. Analyses were performed also at 15 kV accelerating voltage. The SEM was operated with a resolution of 0.8 nm and a probe current of 1.6 nA. A count time of 100 s was used for punctual analyses. Total chemical composition was expressed on the basis that the sum of oxide mass equals 100 for determinations of SiO$_2$, Al$_2$O$_3$, Fe$_2$O$_3$, MgO, CaO, K$_2$O, and Na$_2$O and TiO$_2$ (Bruand et al., 2022; 2023; Bruand and Reatto, 2022). The detection
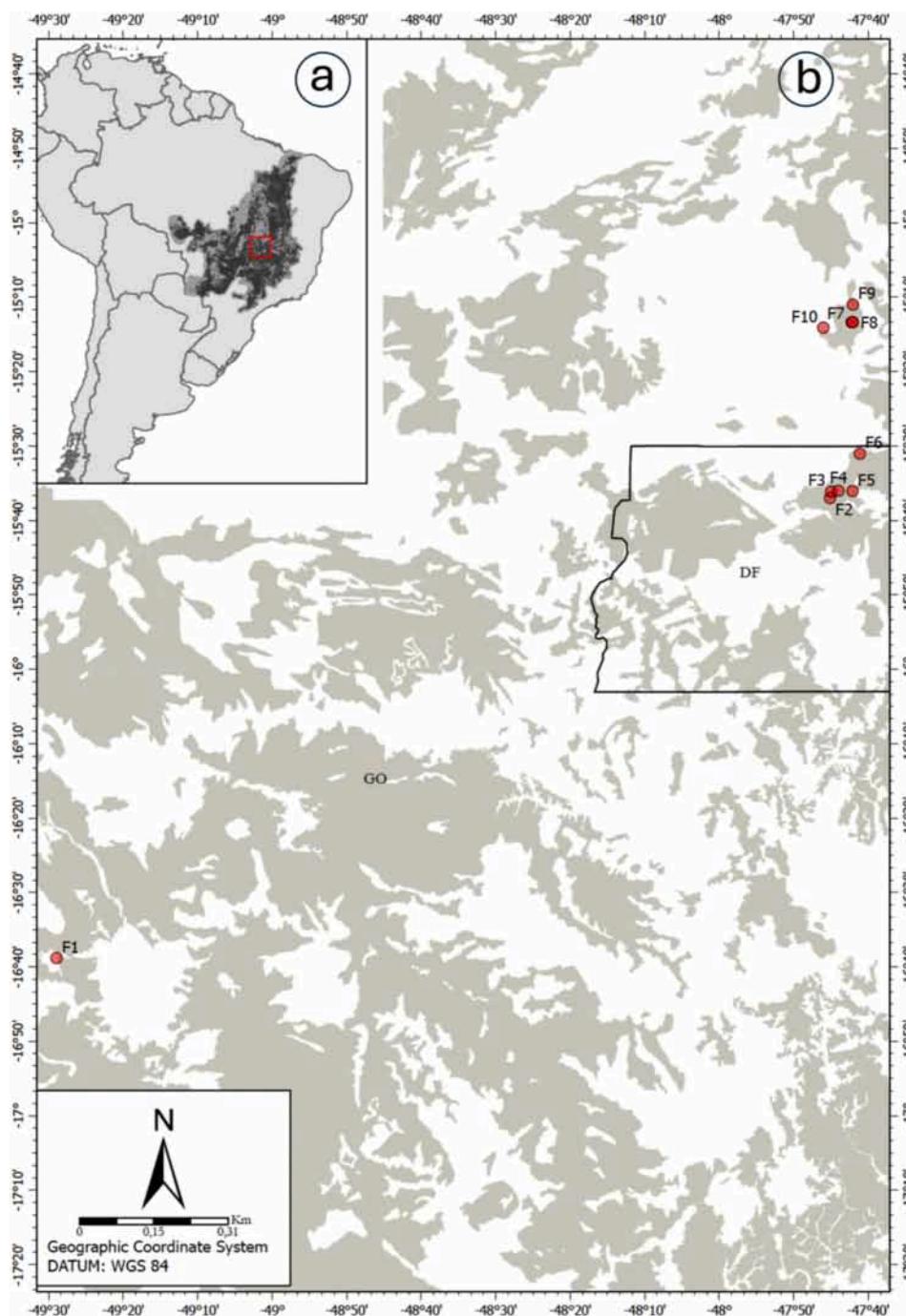
Fig. 1. Extension of the Cerrado region (a) and location of the Ferralsols studied (F1 to F10) (b). The grey areas in (b) correspond to areas with Ferralsols (DF: District Federal; GO: state of Goiás).

limit of oxide content was estimated at 0.01 %. The number of elongated particles with an internal sheet structure and K_2O content higher than 0.5 % was determined by eye on the polished sections 4.9 cm^2 in surface area at varying magnifications using BESIs distributed on the whole cross section. Images of the concentration of K throughout the images were recorded with an acquisition time of 5 min. As the total chemical compositions recorded for the phyllosilicates particles with a K_2O content higher than 7 % were close to those of dioctahedral 2:1 phyllosilicates, the structural model of the half unit cell of such minerals was used to compute the structural formuæ (Aurousseau et al., 1983; Crowley, 1991). According to that structural model, the whole Si^{4+} was located in the tetrahedral cavities and then supplemented by Al^{3+} in such a way as to occupy the four tetrahedral cavities per half unit cell. Then, the

remaining Al^{3+} was located in the octahedral cavities. All the Fe^{3+}, Mg^{2+} and Ti^{4+} were also located in the octahedral cavities. In accordance with the structural model used, the entire K^+, Na^+ and Ca^{2+} were located in the inter-layer space to equilibrate the negative charge of the layer. The latter result from the balance of the negative charges related to O^{2-} and OH^- whose packing defines the tetrahedral and octahedral cavities, and of the positive charges related to Si^{4+} and Al^{3+} in the tetrahedral cavities and to Al^{3+}, Mg^{2+} and Ti^{4+} in the octahedral cavities (Aurousseau et al., 1983; Crowley, 1991). All the analyses carried out using EDS on particles of phyllosicates with K_2O content less than 7 % were discarded because most of them corresponded to small particles for which part of the material surrounding the particle might have been included in the volume analyzed, thus possibly explaining the low K_2O

Table 1

Main physico-chemical characteristics of the ferralic B horizons (FB) studied (modified after Reatto et al., 2007 and 2008).

Soil	Coordinates	Depth	Saprolite Depth	Type of parent material	Particle size distribution			pH$_w$	Organic carbon content	Bulk density
					Clay	Silt	Sand			
		Cm	Cm		%	%	%		g kg^{-1}	
FB1	S 16°38′50.84″ W 49°28′59.84″	100–160	350–400	Precambrian mafic granulite	52	4	44	5.34	0.34	1.21
FB2	S 15°37′1.27″ W 47°45′5.76″	115/120–200+	200–400	Precambrian sandy metarythmite	61	14	25	5.3	0.61	0.9
FB3	S 15°36′9.19″ W 47°45′0.78″	130–180	200–400	Precambrian sandy metarythmite	75	9	16	5.2	0.02	0.88
FB4	S 15°36′3.20″ W 47°44′1.48″	60–110	200–250	Precambrian quartzite	30	1	69	5.24	0.34	1.18
FB5	S 15°36′5.02″ W 47°42′8.13″	57/90–90/120	200–800	Precambrian clayed metarythmite	55	15	30	4.8	0.62	1.02
FB6	S 15°31′4.50″ W 47°41′9.03″	140–200+	500–600	Precambrian metapelite	78	9	13	4.8	0.02	0.83
FB7	S 15°13′24.20″ W 47°42′14.70″	96/110–200+	200–300	Precambrian metapelite	70	14	16	4.8	0.59	0.96
FB8	S 15°13′23.30″ W 47°42′5.20″	95–200+	200–300	Precambrian metapelite	76	7	17	4.9	0.61	0.98
FB9	S 15°11′1.83″ W 47°43′6.80″	100/110–180	200–400	Precambrian metapelite and limestone	75	8	17	5	0.01	1.06
FB10	S 15°14′8.00″ W 47°46′3.72″	100–140	200–400	Tertiary lacustrine limestone	75	7	18	5.2	0.02	0.88

pH$_w$: pH in water.

Table 2

Main minerals present in the ferralic B horizons studied after Reatto (2009) modified.

Soil	Kaolinite	Gibbsite	Hematite	Goethite
	g kg^{-1}			
FB1	196	539	205	60
FB2	320	496	142	42
FB3	412	442	0	146
FB4	197	625	0	178
FB5	619	201	139	41
FB6	442	365	137	56
FB7	591	241	75	93
FB8	605	218	137	40
FB9	645	183	133	39
FB10	399	405	196	0

Table 3

Total K$_2$O content (mass % of total oxides) measured using ICP-AES (a) after extraction with fluorohydric and perchloric acids (see Table SD1, Supplementary Data) and using EDS (b) on areas (1000 × 1200 μm^2) of the polished cross sections (see Table SD2, Supplementary Data) in the ferralic B horizons studied.

Soil	K$_2$O Mass %	
	(a)	(b)
FB1	0.13	0.24
FB2	0.04	0.02
FB3	0.05	0.08
FB4	0.03	0.03
FB5	0.20	0.15
FB6	0.07	0.11
FB7	0.19	0.21
FB8	0.18	0.20
FB9	0.67	0.76
FB10	0.21	0.18

content.

3. Results and discussion

3.1. Total K content

Table 3 shows that total K$_2$O content, as determined through chemical extraction, varied from 0.02 % (FB) to 0.67 % (FB9) of the mass of oxides (Table SD1, Supplementary Data). However, when measured using EDS on areas of the polished cross sections, the range extended from 0.03 % (FB4) to 0.76 % (FB9) of the mass of oxides (Table SD2, Supplementary Data). While differences were measured between the two methods, the variation of total K$_2$O content remained consistent across the ferralic B horizons analyzed. As the total K$_2$O content measured after chemical extraction on bulk sieved samples is considered as the reference method, our results recorded using EDS on polished cross sections could reasonably be considered representative of the total K$_2$O content in the different ferralic B horizons studied (Table 3). While numerous studies have been conducted on the total K content in topsoils of Ferralsols (e.g. Darunsontaya et al., 2012; Firmano et al., 2020; Marchi et al., 2012; Moterle et al., 2016; 2019; Poss et al., 1991; Tawornpruek et al., 2006; Volf et al., 2023), there is a dearth of information on the quantity of K in their B horizons. The total K$_2$O contents recorded in the ferralic B horizons studied were very high compared to those recorded earlier by Moterle et al. (2016) who reported K$_2$O = 0.01 % of the mass of the oven-dried soil without any K fertilization, and by Marchi et al. (2012) who found K$_2$O < 0.01 % of the mass of the oven-dried soil in Brazilian ferralic B horizons developed on basalts without any K fertilization (Table 3). Our smallest K$_2$O contents were of the same order of magnitude as those recorded in Brazilian ferralic B horizons developed on gneiss and pellitic rocks (Silva et al., 2000), namely a K$_2$O content ranging from 0.02 to 0.05 % of the mass of the oven-dried soil without any K fertilization. They were also close to those recorded in the Togolese ferralic B horizons studied by Poss et al. (1991) who reported K$_2$O = 0.06 % of the mass of the oven-dried soil ferralic B horizons. Finally, Darunsontaya et al. (2012) recorded a range of K$_2$O content in Thai ferralic B horizons developed on a large range of parent materials close to that recorded for the ferralic B horizons studied, with a K$_2$O content ranging from 0.04 to 0.28 % of the mass of the oven-dried soil without any K fertilization.

3.2. K-bearing phyllosilicates

Using BESI polished cross-sections and EDS analyses, we observed the presence of elongated K-bearing particles of varying sizes in the ferralic B horizons studied (Figs. 2 to 4). Results recorded using EDS showed that K was only detected in these elongated particles. Their length ranged from 1 to 800 μm with numerous very small particles < 2 μm in length in FB6 and FB9 and numerous large particles 50 to 800 μm in length in FB1 (Table 4, Fig. 2). They were present in all the ferralic B horizons studied (Table 4). In FB2, FB3 and FB4 they were mostly < 2

μm in length and not numerous (Fig. 3) whereas in FB5, FB7, FB8 and FB10 they were numerous with a length < 2 μm or from 2 to 20 μm (Table 4, Fig. 4).

The structural formula computed for the elongated particles analyzed showed that most, if not all, of the positive electrical charge in the inter-layer space corresponded to K^+ with a mean number of K^+ atoms ranging from 0.69 to 0.85 per half-unit-cell of the structural formula (Table 5), whereas it ranged from 0.54 to 0.96 for the particles analyzed by half-unit-cell of the structural formula (Table SD3, Supplementary Data). Results also showed that from 14 to 28 % of the
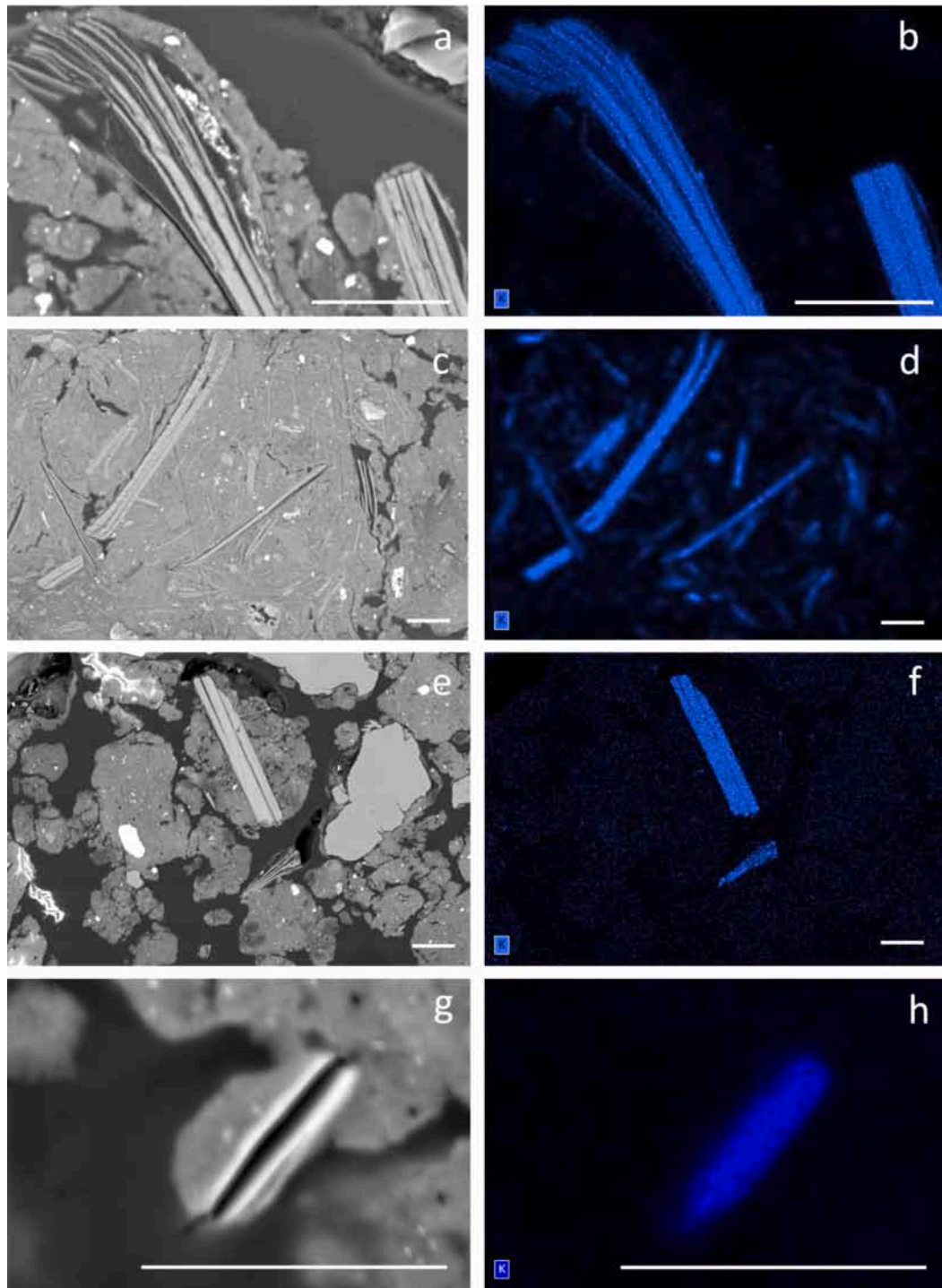
Fig. 2. Elongated particles with varying sizes observed on the backscattered scanning images (BESI) of the cross sections of FB1 (a, c and e) and FB3 (g) and corresponding K maps of the same areas using EDS for FB1 (b, d and f) and FB3 (h). Bar length: 20 μm.
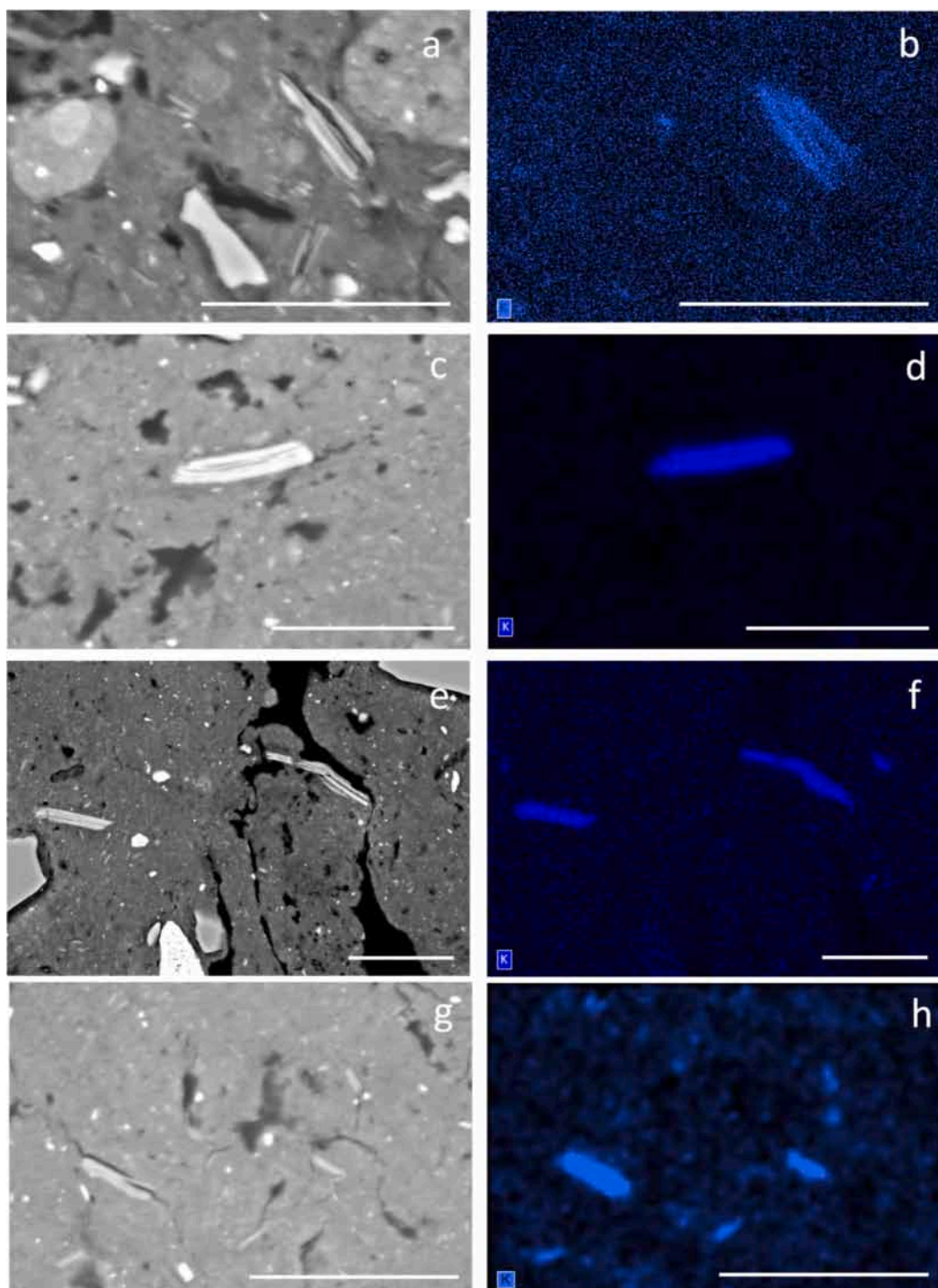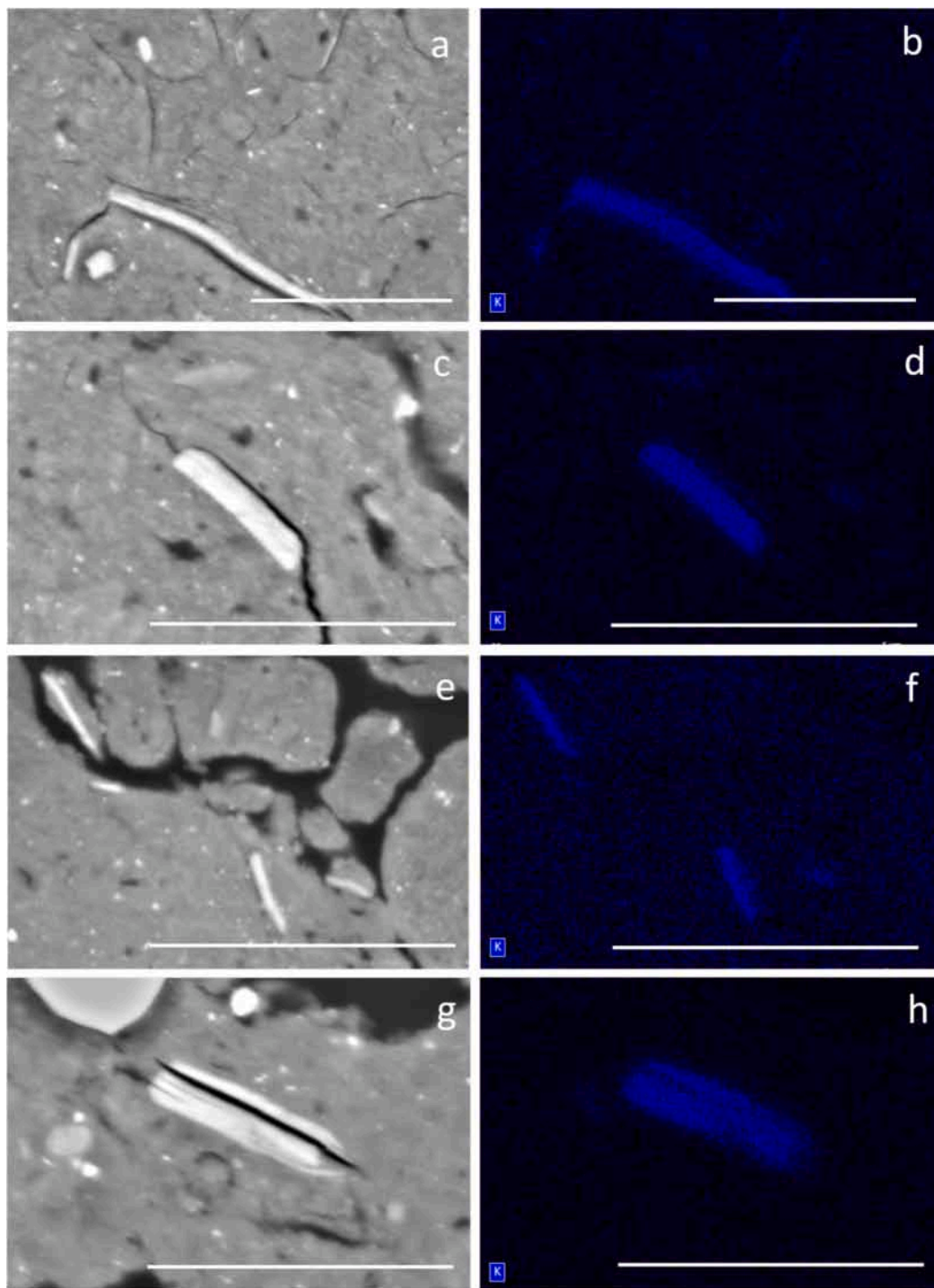
Fig. 3. Elongated particles with varying sizes observed on the backscattered scanning images (BESI) of the cross sections of FB5 (a, and c), FB7 (e) and FB9 (g) and corresponding K maps of the same areas using EDS for FB5 (b and d), FB7 (f) and FB9 (h). Bar length: 20 μm.

positive electrical charge in the inter-layer space corresponded to Na$^+$ in FB1 and from 7 to 14 % in FB9 (Table SD3, Supplementary Data). The mean negative electrical charge per half-unit-cell was mainly located in the tetrahedral position. It ranged from −0.87 to −1.03 (Table 5). The mean number of cations in octahedral position per half-unit-cell ranged from 2.02 to 2.10 (Table 5) which is consistent with a dioctahedral 2:1 phyllosilicate. All these characteristics are consistent with a structural formula of poorly weathered muscovite (Aurousseau et al., 1983).

The elongated particles > 50 μm in length observed in FB1 showed Al_2O_3, SiO_2 and K_2O contents close to those of a theoretical muscovite

(Velde and Meunier, 2008) and of a natural muscovite (Aurousseau et al., 1983) (Fig. 5). The highest K_2O contents corresponding to a number of K atoms per half-unit cell ranging from 0.92 to 0.96 in the structural formula were recorded for elongated particles > 20 μm in length in FB2, FB3, FB8 and FB10 (Table SD3, Supplementary Data). In FB1, where the largest elongated particles were observed, the highest K_2O contents recorded were lower because a significant part of the negative charge of the layer was compensated by Na$^+$ (Table SD3, Supplementary Data). Elongated particles from 20 to 50 μm in length and from 2 to 20 μm in length showed a highly varying K_2O content,

Fig. 4. Elongated particles with varying sizes observed on the backscattered scanning images (BESI) of the cross sections of FB9 (a and c) and FB10 (e and g) and corresponding K maps of the same areas using EDS for FB9 (b and d) and FB10 (f and h). Bar length: 20 μm.

some of them showing Al_2O_3, SiO_2 and K_2O contents close to those of a theoretical and natural muscovite (Aurousseau et al., 1983; Velde and Meunier, 2008) and others close to those of a weathered muscovite (Bruand and Reatto, 2022) (Fig. 5, Table SD3, Supplementary Data). Most elongated particles < 2 μm in length showed a much smaller K_2O content than the larger particles (data not published but basic analyses available on demand). This smaller K_2O content can be attributed to both the chemical composition of the elongated particles themselves, and to the inclusion of the surrounding groundmass during the analysis, particularly when dealing with very small particles. All these elongated

K-bearing particles varying in size and chemical composition correspond to 2:1 clay particles ranging from weakly weathered muscovite to hydroxy-Al interlayered vermiculite (HIVs) with part of Al^{3+} located in the inter-layer space instead of the octahedral position as hypothesized for the calculation of the structural formula (Table SD3, Supplementary Data). This will explain the number of octahedral cavities occupied by cations slightly higher than 2 and the deficit of cations in the inter-layer space to equilibrate the negative charge of the layer (Table SD3, Supplementary Data). Our results are consistent with those recorded earlier that were mainly based on X-ray diffraction analysis and which showed

Table 4

Length and number of elongated particles with K_2O content ranging from 0.5 to 12 % which were observed on the backscattered electron scanning images (BESI) of the polished sections 4.9 cm² in surface area (diameter of 2.5 cm) of the ferralic B horizon of the Ferralsols studied. n.o.: not observed (modified after Bruand et al., 2023).

Soil	Number of particles			
	<2 µm	2–20 µm	20–50 µm	>50 µm
FB1	50–100	10–50	10–50	10–50
FB2	10–50	1–10	1–10	n.o.
FB3	10–50	1–10	n.o.	n.o.
FB4	10–50	1–10	n.o.	n.o.
FB5	50–100	50–100	1–10	n.o.
FB6	50–100	10–50	1–10	n.o.
FB7	50–100	50–100	1–10	n.o.
FB8	50–100	50–100	1–10	n.o.
FB9	>100	50–100	10–50	n.o.
FB10	50–100	50–100	n.o.	n.o.

the presence of varying small quantities of micas, vermiculite, illite, and HIVs within the clay and silt fractions in Brazilian Ferralsols (e.g. Bertolazi et al., 2017; Brito Galvão and Schulze, 1996; Caner et al., 2014; Marques et al., 2011; Oliviera et al., 2020; Pacheco et al., 2018).

3.3. Cation exchange capacity and exchangeable cations

Results showed that the cation exchange capacity (CEC) ranged from 0.24 cmol$_+$ kg^{-1} (FB4) to 1.85 cmol$_+$ kg^{-1} (FB9) (Table 6). Soils with a CEC < 1 cmol$_+$ kg^{-1} (FB1, FB2, FB3, FB4 and FB6) were found to be associated to soils with a mass proportion of kaolinite < 0.5 g/g in the clay fraction (Reatto et al., 2009). The smallest CEC (FB4, 0.24 cmol$_+$ kg^{-1}) corresponded to the ferralic B horizon with the smallest clay content (30 %) (Table 1) and the smallest mass proportion of kaolinite in the clay fraction (0.20 g/g) (Reatto et al., 2009). The highest CEC (FB9, 1.85 cmol$_+$ kg^{-1}) corresponded to the ferralic B horizon with one of the highest clay contents (75 %) (Tables 1 and 6) and the highest mass proportion of kaolinite in the clay fraction (0.65 g/g) (Reatto et al.,

2009). The CEC recorded for the ferralic B horizons studied are much lower than the maximum CEC limit (i.e. < 16 cmol$_+$ kg^{-1} when measured at pH 7 according to the ISS Working Group WRB, 2022) not to be exceeded for a ferralic horizon. This observation can be attributed to the measurement of the CEC at the soil pH close to 5, which allows us to exclude the contribution of negative charges that appear at pH 7. Indeed, the minerals of these soils are known to exhibit variable surface electrical changes depending on the pH (Julien et al., 2023; Qafoku et al., 2004).

Results also show that the amount of exchangeable Al^{3+} represented between 77 (FB9) and 99 % (FB2) of the exchangeable cations except for FB1 (46 %) and FB10 (50 %) (Table 6). The five ferralic B horizons with a content in exchangeable Al^{3+} >1.3 cmol$_+$ kg^{-1} corresponded to those with pH < 5 (Tables 1 and 6). In FB1, the high content of exchangeable Ca^{2+} (0.052 cmol$_+$ kg^{-1}), exchangeable Mg^{3+} (0.098 cmol$_+$ kg^{-1}) and exchangeable K^+ (0.022 cmol$_+$ kg^{-1}) can be related to the mafic character of the parent material (Table 1). As for FB10, the relatively high content in exchangeable Ca^{2+} (0.290 cmol$_+$ kg^{-1}), exchangeable Mg^{2+} (0.544 cmol$_+$ kg^{-1}) and exchangeable K^+ (0.029 cmol$_+$ kg^{-1}) are related to the calcareous character of the parent material which is lacustrine limestone (Table 1). This high proportion of the exchangeable cations Ca^{2+}, Mg^{2+} and K^+ among the exchangeable cations indicates that in these soils under native vegetation, although they result from a very long geochemical evolution and the depth of appearance of the saprolite varies from 200 to 800 cm (Table 1), the state of saturation of the cation exchange capacity remains influenced by the geochemical characteristics of the parent material. This influence can be attributed to the burrowing activity of termites, as evidenced by Bruand et al. (2022, 2023) in the same ferralic B horizons. Since ferralsols are geochemically highly depleted soils, termites transport specific soil material upward from the saprolite, which contains clay material and cations that are encountered only at depth, close to this soil layer. Clay minerals are crucial for the construction of termite nests (Jouquet et al., 2004, 2016), while cations, especially Na+, are considered limiting factors for decomposers (Jouquet and Bruand, 2023).

When it was higher than the limit of detection (i.e. > 0.02 cmol$_+$

Table 5

Averaged structural formulæ computed for elongated particles showing a K_2O content > 7 % in every ferralic B horizon studied (see Table SD3, Supplementary Data). X, number of octahedral cavities occupied per half-unit-cell (X = c + d + e + f); Y, sum of the charges of the cations in the inter-layer space (Y = g + (2 × h) + f). Elementary results are given in Table SD3 (Supplementary Data). Structural formulae for a theoretical muscovite (Velde and Meunier, 2008) and a muscovite of a granite (Aurousseau et al., 1983) are also given.

Soil		$\left[Si_a^{4+}Al_b^{3+}\right]O_{10}^{2-}\left[Al_c^{3+}Fe_d^{3+}Mg_e^{2+}Ti_f^{4+}\right](OH)_2^- K_g^+Ca_h^{2+}Na_i^+$										
		A	b	c	d	e	f	g	h	i	X	Y
FB1	Mean	3.05	0.95	1.77	0.14	0.08	0.04	0.69	0.01	0.20	2.03	0.91
	s.d.	0.05	0.05	0.04	0.03	0.04	0.01	0.06	0.01	0.05	0.03	0.07
FB2	Mean	3.03	0.97	1.76	0.18	0.09	0.03	0.83	0.00	0.03	2.06	0.86
	s.d	0.03	0.03	0.03	0.03	0.04	0.02	0.17	0.01	0.02	0.05	0.16
FB3	Mean	2.97	1.03	1.77	0.18	0.07	0.04	0.83	0.01	0.04	2.05	0.88
	s.d.	–	–	–	–	–	–	–	–	–	–	–
FB4	Mean	2.98	1.02	1.74	0.22	0.09	0.03	0.82	0.01	0.03	2.08	0.86
	s.d.	–	–	–	–	–	–	–	–	–	–	–
FB5	Mean	3.05	0.95	1.70	0.23	0.14	0.04	0.69	0.01	0.10	2.10	0.80
	s.d.	–	–	–	–	–	–	–	–	–	–	–
FB6	Mean	3.06	0.94	1.79	0.16	0.09	0.03	0.73	0.00	0.07	2.07	0.79
	s.d.	0.08	0.08	0.04	0.02	0.04	0.01	0.05	0.00	0.05	0.01	0.03
FB7	Mean	3.06	0.94	1.64	0.29	0.12	0.03	0.74	0.01	0.02	2.08	0.79
	s.d	0.05	0.05	0.07	0.06	0.03	0.02	0.06	0.01	0.01	0.04	0.06
FB8	Mean	3.00	0.99	1.77	0.22	0.06	0.02	0.80	0.01	0.04	2.07	0.85
	s.d.	0.04	0.03	0.11	0.09	0.03	0.01	0.11	0.01	0.02	0.01	0.11
FB9	Mean	3.09	0.91	1.79	0.15	0.08	0.03	0.74	0.01	0.08	2.05	0.84
	s.d.	0.06	0.06	0.07	0.03	0.03	0.02	0.12	0.01	0.02	0.03	0.10
F10	Mean	3.13	0.87	1.64	0.24	0.13	0.01	0.87	0.01	0.02	2.02	0.90
	s.d.	–	–	–	–	–	–	–	–	–		
All particles together	Mean	3.05	0.95	1.75	0.18	0.09	0.03	0.75	0.01	0.10	2.05	0.86
	s.d.	0.06	0.06	0.08	0.07	0.04	0.01	0.10	0.01	0.09	0.04	0.09
Theoretical muscovite		3.00	1.00	2.00	0.00	0.00	0.00	1.00	0.00	0.00	2.00	1.00
Muscovite in a granite		3.16	0.84	1.66	0.07	0.28	0.05	0.95	0.00	0.00	2.01	0.95
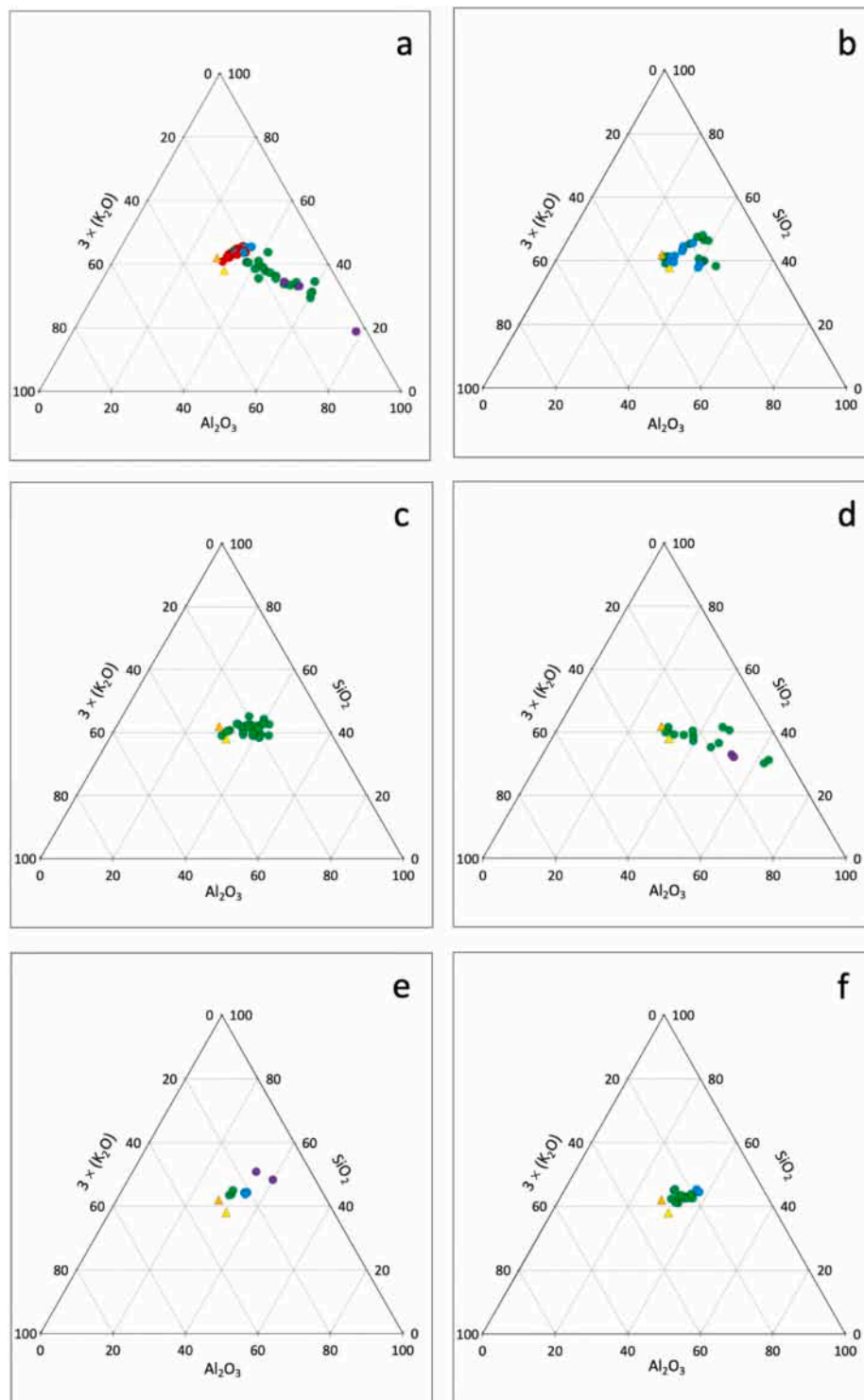
Fig. 5. Respective content in Al$_2$O$_3$, SiO$_2$ and K$_2$O in the elongated particles varying in size (red circles: > 50 μm; blue circles: 20–50 μm; green circles: 2–20 μm; purple circles: < 2 μm) in the different ferralic B horizons studied (FB1: a, FB2: b, FB3: c, FB4: d, FB5: e, FB6: f, FB7: g, FB8: h, FB9: i and FB10: j). Theoretical composition of muscovite (orange triangle) (Meunier and Velde, 2008) and composition of muscovite particles (yellow triangle) (Aurousseau et al., 1983) are also plotted. (For interpretation of the references to colour in this figure legend, the reader is referred to the web version of this article.)

kg^{-1} in FB1, FB5, FB7, FB9 and FB10, Table 6), the exchangeable K$^+$ content in the ferralic horizons studied was much smaller than those recorded in the Ferralsols studied by Volf et al. (2023). The latter were developed on a large range of parent materials and the exchangeable K$^+$ content ranged from 0.100 to 0.828 cmol$_+$ kg^{-1} but these Ferralsols were mostly located in cultivated land and the samples analyzed were collected at depths of 0–20 cm or 20–40 cm. A similar comparison can be made under native vegetation with the exchangeable K$^+$ contents measured by Moterle et al. (2016) in a Brazilian Ferralsol with an exchangeable K$^+$ content of 0.128 cmol$_+$ kg^{-1} in the 0–10 cm horizon. On the other hand, the exchangeable K$^+$ content in the ferralic B horizons studied was close to those measured by Firmano et al. (2020) at
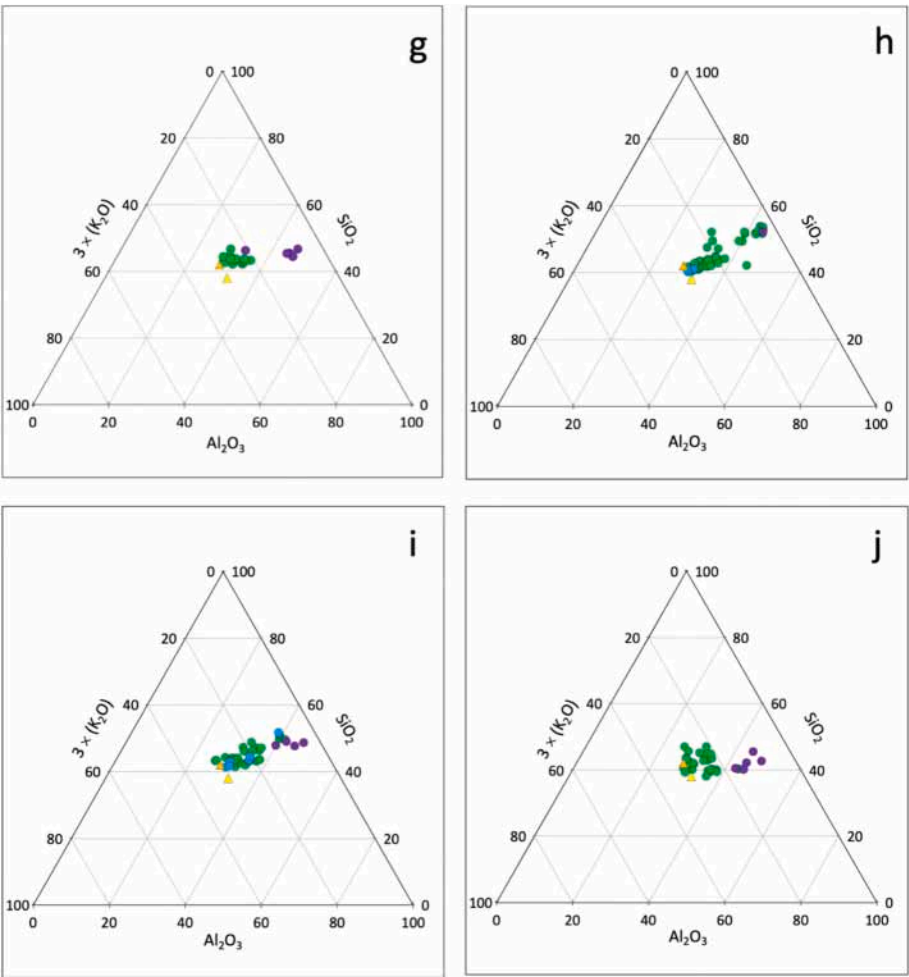
Fig. 5. (*continued*).

Table 6
Cation exchange capacity (CEC) and exchangeable cations determined at the pH of the soil for the ferralic B horizons studied.

Soil	CEC	Exchangeable cations					
		Ca^{++}	Mg^{++}	K^+	Na^+	Al^{+++}	H^+
	$cmol_+ \ kg^{-1}$	$cmol_+ \ kg^{-1}$					
FB1	0.51	0.052	0.098	0.022	<0.005	0.135	<0.05
FB2	0.66	<0.04	0.006	<0.02	<0.005	0.460	<0.05
FB3	0.72	0.080	0.011	<0.02	<0.005	0.787	0.071
FB4	0.24	<0.04	0.007	<0.02	<0.005	0.659	0.101
FB5	1.82	<0.04	0.040	0.053	0.008	1.319	0.142
FB6	0.66	<0.04	0.012	<0.02	<0.005	1.477	0.112
FB7	1.14	<0.04	0.040	0.029	0.006	1.589	0.122
FB8	1.48	<0.04	0.019	<0.02	0.010	1.499	0.172
FB9	1.85	<0.04	0.018	0.032	<0.005	0.816	0.193
FB10	1.28	0.290	0.544	0.029	0.009	1.281	0.133

depths of 0–20 cm or 20–40 cm in Brazilian Ferralsols under native vegetation developed on basalts. It was also close to those measured in the ferralic B horizons of Togolese Ferralsols under native vegetation and culture and developed on Tertiary alluvial deposits which ranged from 0.026 to 0.074 $cmol_+ \ kg^{-1}$ (Poss et al., 1991), to those recorded in Thai Ferralsols developed on Permian calcareous sedimentary rocks which ranged from 0.010 to 0.100 $cmol_+ \ kg^{-1}$ (Tawornpruek et al., 2006), and to those of a cultivated Brazilian Ferralsol developed on a basalt with the exchangeable K^+ content of 0.076 $cmol_+ \ kg^{-1}$ (Marchi et al., 2012).

3.4. Total and exchangeable K stocks

The stocks of total and exchangeable K, expressed in kg ha^{-1} for ferralic B horizons 1 m thick, were compared (Table 7). For the ferralic B horizons for which the exchangeable K^+ content was higher than the detection limit, it ranged from 7.9 % (FB2) to 13.5 % (FB5) of the total K content except for FB9 in which it corresponded to only 2.5 % of the total K content, the latter being the highest for the horizons studied (Table 7). On the other hand, the not measurable exchangeable K^+ contents (FB2, FB3, FB4, FB6 and FB8) corresponded to the smallest total K contents recorded except for FB8, thus indicating that the exchangeable K^+ content for that horizon may be close to the detection

Table 7
Stock of total K measured using ICP-AES after extraction with fluorohydric and perchloric acids and stock of exchangeable K^+ measured using cobaltihexamine.

Soil	Total K	Total exchangeable K^+
	kg $ha^{-1} \ m^{-1}$	
FB1	1095	86
FB2	259	<18
FB3	269	<18
FB4	310	<18
FB5	1529	207
FB6	363	<18
FB7	1231	125
FB8	1237	<18
FB9	5044	125
FB10	1209	113

limit. This relationship between the quantities of total K and exchangeable K^+ in the different horizons studied show that the exchangeable K^+ appears to be related to the distribution of the elongated particles, as the latter are the only K-bearing minerals with a K content higher than the detection limit identified in the horizons as mentioned above. All the horizons with an exchangeable K^+ higher than the detection limit (>18 kg ha^{-1} m^{-1}) did indeed show the presence of 10 to 50 elongated particles 2–20 μm in length and at least 10 to 50 elongated particles < 2 μm in length in the areas studied on the BESI.

As discussed above, the stock of total K appears to be related to the density of elongated particles < 2 μm and 2–20 μm in length. When there were fewer than 50 elongated particles < 2 μm and 2–20 μm in length in the polished section observed, the stock of total K was smaller than 100 kg ha^{-1} m^{-1} (Table 7). On the other hand, while the CEC appeared to be mainly related to the clay content and the proportion of kaolinite in the clay fraction as discussed above, the stock of exchangeable K^+ appears to be related also, as shown for the total K content, to the density of elongated particles < 2 μm and 2–20 μm in length as it ranged from 86 to 207 kg ha^{-1} m^{-1} in the horizons with a content in elongated particles < 2 μm and 2–20 μm in length higher than 50. The horizon FB8 was however an exception because although it satisfied the rule on both the size and number of elongated particles, the stock of exchangeable K^+ was too low to be measured and, as for FB2, FB3, FB4 and FB6, it was thus smaller than 18 kg ha^{-1} m^{-1}.

The presence of 10 to 50 elongated particles > 50 μm in length in FB1 did not seem to influence the exchangeable K^+ content; likewise, the presence of 10 to 50 elongated particles 20–50 μm in length in FB1 and FB9 did not seem to influence the exchangeable K^+ content. This can be related to the low availability of K^+ located in the inter-layer space because of the high negative electrical charge of the layers (Table SD3, Supplementary Data).

Recent studies (Bruand et al., 2022; 2023; Bruand and Reatto, 2022) have discussed the presence of elongated particles corresponding to K-bearing 2:1 phyllosilicates at varying degrees of weathering in Ferralsols. As mentioned above regarding the nature of exchangeable cations and the characteristics of the parent material of the Ferralsols studied, the presence of these particles can be explained by the burrowing activity of social insects, particularly termites, which are abundant in the study fields (Reatto et al., 2009). In this environment, termites are considered to be responsible for transporting material upward from the saprolite. This raises the question about the role of these insects in controlling the availability of K^+ for plant nutrition and total K potentially available (Barros et al., 2001; Benito et al., 2004; Black and Okwakol, 1997; Decaens et al., 1994). These studies which reported that native vegetation clearing followed by cultivation usually reduces biodiversity, with the diversity and density of termite populations being particularly affected, do indeed question the renewal in the ferralic B horizons of the stock of the reserve of K and of the part of K which was available for plant nutrition under native vegetation. Yet again, the question of the consequences of cultivation on soil fauna and the resulting evolution of the physical and chemical properties arises (Bruand, 2023; Galindo et al., 2022; Lavelle et al., 2020).

4. Conclusions and implications

Our results showed that the total K and exchangeable K^+ were related to the presence of elongated particles corresponding to 2:1 phyllosilicates at varying degrees of weathering in all the ferralic B horizons studied. These 2:1 phyllosilicates ranged from weakly weathered muscovite to HIV. The quantities of K reserve potentially available over time for plant nutrition according to the physico-chemical conditions prevailing in these soils appeared to be close to those recorded in several other countries for Ferralsols where 2:1 phyllosilicates were identified using mainly X-ray diffraction without further analysis. The stock of exchangeable K^+ was related to the density of the elongated particles < 2 μm and 2–20 μm in length because their K was more

exchangeable than in the larger particles. The CEC varied according to the clay content and the kaolinite proportion in the clay fraction.

Furthermore, recent research indicates that these K-bearing elongated particles consisting of 2:1 phyllosilicates result from the translocation activities of social insects, particularly termites, which transport material from the saprolite up to the surface. It is therefore increasingly important to assess the impact of soil cultivation on the soil fauna. This is crucial as it directly influences the K reserves and its bioavailability for plant nutrition, raising substantial issues for agricultural practices and soil management. Notably, when Ferralsols under natural vegetation are cleared for cultivation, the resulting impact on the social insect populations, which play a pivotal role in maintaining soil health and fertility, must be accounted for. Disruption to these populations could compromise the K cycle in these soils, ultimately challenging the assumption of available K for future agricultural use. It is essential to understand that the actions of soil-dwelling fauna, particularly in the context of land use change, have far-reaching implications for nutrient dynamics and soil conservation.

CRediT authorship contribution statement

Ary Bruand: Writing – review & editing, Writing – original draft, Validation, Resources, Methodology, Investigation, Funding acquisition, Formal analysis, Data curation, Conceptualization. **Michel Brossard:** Writing – review & editing, Validation, Methodology, Investigation. **Pascal Jouquet:** Writing – review & editing, Validation, Methodology. **Adriana Reatto:** Writing – review & editing, Validation, Resources, Methodology. **Jérémie Garnier:** Writing – review & editing, Validation, Methodology. **Julia Mancano Quintarelli:** Writing – review & editing. **Éder de Souza Martins:** Writing – review & editing, Validation.

Declaration of competing interest

The authors declare that they have no known competing financial interests or personal relationships that could have appeared to influence the work reported in this paper.

Data availability

The datasets used during the current study are available from the corresponding author on request.

Appendix A. Supplementary data

Supplementary data to this article can be found online at https://doi.org/10.1016/j.geoderma.2024.116949.

References

AFES, 2008. Référentiel pédologique. Association française pour l'étude du sol (AFES). Éditions Quæ, Versailles, p. 405 p..

Agbenin, J.O., van Raij, B., 1999. Rate processes of calcium, magnesium and potassium desorption from variable-charge soils by mixed ion-exchange resins. Geoderma 93 (1–2), 141–157. https://doi.org/10.1016/S0016-7061(99)00049-X.

Almeida, C.C., Fontes, M.P.F., Dias, A.C., Pereira, T.T.C., Ker, J.C., 2021. Mineralogical, chemical and electrochemical attributes of soils. Sci. Agric. 78, e20200071.

Andrist-Rangel, Y., Edwards, A.C., Hillier, S., Öborn, I., 2007. Long-term K dynamics in organic and conventional mixed cropping systems as related to management and soil properties. Agr. Ecosyst. Environ. 122, 413–426. https://doi.org/10.1016/j.agee.2007.02.007.

Aurousseau, P., Curmi, P., Bouille, S., Charpentier, S., 1983. Les vermiculites hydroxy-alumineuses du Massif Armoricain (France). Approche minéralogique, microanalytique et thermodynamique. Geoderma 31, 17–40. https://doi.org/10.1016/0016-7061(83)90081-2.

Barros, E., Curmi, P., Hallaire, V., Chauvel, A., Lavelle, P., 2001. The role of macrofauna in the transformation and reversibility of soil structure of an oxisol in the process of forest to pasture conversion. Geoderma 100, 193–213. https://doi.org/10.1016/S0016-7061(00)00086-0.

Bell, M.J., Ransom, M.D., Thompson, M.L., Hinsinger, P., Florence, A.M., Moody, P.W., Guppy, C.N., 2021. Considering soil potassium pools with dissimilar plant availability. In: Murell, T.S., Mikkelsen, G.S., Norton, R., Thompson, M.L. (Eds.), Improving Potassium Recommendations for Agricultural Crops. Springer Verlag, New York, pp. 163–190.

Benito, N.P., Broassard, M., Pasini, A., Guimarães, M.F., Bobillier, B., 2004. Transformations of soil macroinvertebrates populations after native vegetation conversion to pasture cultivation (Brazilian Cerrado). Eur. J. Soil Biol. 40, 147–154. https://doi.org/10.1016/j.ejsobi.2005.02.002.

Bertolazi, V.T., Inda, A.V., Caner, L., Martins, A.P., Vaz, M.A.B., Bonnet, M., Anghinoni, I., Carvalho, P.C.F., 2017. Impact of an integrated no-till soybean-beef cattle production system on Oxisol mineralogy in southern Brazil. Appl. Clay Sci. 149, 67–74. https://doi.org/10.1016/j.clay.2017.08.028.

Black, H.I.J., Okwakol, M.J.N., 1997. Agricultural intensification, soil biodiversity and agroecosystem function in the tropics: the role of termites. Appl. Soil Ecol. 6, 37–53. https://doi.org/10.1016/S0929-1393(96)00153-9.

Boeira, R.C., van Raij, B., Silva, A.S., Maximiliano, V.C.B., 2004. Simultaneous extraction of aluminum, calcium, magnesium, potassium, and sodium with ammonium chloride solution. Rev. Bras. S. Do Solo 28 (5), 929–936. https://doi.org/10.1590/S0100-06832004000500015.

Bortolon, L., Gianello, C., Schlindwein, J.A., 2010. Available potassium in soils of Southern Brazil estimated by multielement methods. Revista Brasileira De Cienca Do Solo 34, 1753–1761. https://doi.org/10.1590/S0100-06832010000500027.

Bortoluzzi, E.C., Velde, B., Pernes, M., Dur, J.C., Tessier, D., 2008. Vermiculite, with hydroxy-aluminium interlayer, and kaolinite formation in a subtropical sandy soil from south Brazil. Clay Miner. 43, 185–1993. https://doi.org/10.1180/claymin.2008.043.2.03.

Brito Galvão, T.C.D., Schulze, D.G., 1996. Mineralogical properties of a collapsible lateritic soil from Minas Gerais. Brazil. Soil Sci. Soc. Am. J. 60, 1969–1978. https://doi.org/10.2136/sssaj1996.03615995006000060050x.

Bruand, A., 2023. Social insects behind the microgranular structure of Ferralsols: consequences for their physical fertility. Pedosphere. https://doi.org/10.1016/j.pedsph.2023.12.011.

Bruand, A., Cousin, I., Nicoullaud, B., Duval, O., Bégon, J.C., 1996. Backscattered electron scanning images of soil porosity for analyzing soil compaction around roots. Soil Sci. Soc. Am. J. 60, 895–901. https://doi.org/10.2136/sssaj1996.03615995006000030031x.

Bruand, A., Reatto, A., 2022. Morphology, chemical composition and origin of 2:1 phyllosilicates in Bw horizons of latosols of the Brazilian Central Plateau: contribution to the discussion of the microgranular structure origin. C.R. Geosc. 354, 159–185. https://doi.org/10.5802/crgeos.123.

Bruand, A., Reatto, A., Martins, E.D.S., 2022. Allochthonous material originating from saprolite as a marker of termite activity in Ferralsols. Sci. Rep. 12, 17193. https://doi.org/10.1038/s41598-022-21613-6.

Bruand, A., Reatto, A., Brossard, M., Jouquet, P., Martins, E.D.S., 2023. Long-term activity of social insects responsible for the physical fertility of soils in the tropics. Sci. Rep. 13, 12337. https://doi.org/10.1038/s41598-023-39654-w.

Caner, L., Radtke, L.M., Vignol-Lelarge, L.M., Inda Jr, A.V., Bortoluzzi, E.C., Mexias, A.S., 2014. Basalt and rhyo-dacite weathering and soil clay formation under subtropical climate in southern Brazil. Geoderma 235–236, 100–112. https://doi.org/10.1016/j.geoderma.2014.06.024.

Chesworth, W., 2008. Potassium Cycle. In: Chesworth, W. (Ed.), Encyclopedia of Soil Science. Springer, p. 902 p.. ISBN 978-1-4020-5127-2.

Ciesielski, H., Sterckeman, T., 1997. A comparison between three methods for the determination of cation exchange capacity and exchangeable cations in soils. Agronomie 17, 9–16. https://doi.org/10.1051/agro:19970102.

Crowley, S.F., 1991. Diagenetic modification of detrital muscovite: an example from the great limestone cyclothem (Carboniferous) of CO. Durham, UK. Clay Minerals 26, 91–103.

Da Silva, I.R., Neto, A.E.F., Fernandes, L.A., Curi, N., do Vale, F.R., 2000. Forms, quantity/intensity ratio and bioavailibity of potassium in different Latosols (oxisols). Pesquisa Agropecaria Brasileira 35, 2065–2073.

Darunsontaya, T., Suddhiprakan, A., Kheoruenromne, I., Prakongkep, N., Gilkes, R.J., 2012. The forms and availability to plants of soil potassium as related to mineralogy for upland Oxisols and Ultisols from Thailand. Geoderma 170, 1–14. https://doi.org/10.1016/j.geoderma.2011.10.002.

Decaens, T., Lavelle, P., Jimenez, J.J., Escobar, G., Rippstein, G., 1994. Impact of land management on soil macrofauna in the Oriental Llanos of Colombia. Eur. J. Soil Biol. 30, 157–168.

Embrapa, 2006. Sistema Brasileiro de Classificação de Solos. Empresa Brasileira de Pesquisa Agropecuária, Rio de Janeiro-RJ. 306 p.

Firmano, R.F., Melo, V., Montes, C.R., Oliveira, A., Castro, C., Alleoni, L.R.F., 2020. Potassium reserves in the clay fraction of a tropical soil fertilized for three decades. Clays Clay Min. 68, 237–249. https://doi.org/10.1007/s42860-020-00078-6.

Furian, S., Barbiéro, L., Boulet, R., Curmi, P., Grimaldi, M., Grimaldi, C., 2002. Distribution and dynamic of gibbsite and kaolinite in an Oxisol of Serra do Mar, southeastern Brazil. Geoderma 106, 83–100. https://doi.org/10.1016/S0016-7061(01)00117-3.

Galindo, V., Giraldo, C., Lavelle, P., Almbrecht, I., Fonte, S.J., 2022. Land use conversion to agriculture impacts biodiversity, erosion control, and key soil properties in an Andean watershed. Ecosphere 3979. https://doi.org/10.1002/ecs2.3979.

Goldstein, J.I., Newbury, D.E., Michael, J.R., Ritchie, N.W.M., Scott, J.H.J., Joy, D.C., 2018. Scanning electron microscopy and X-ray microanalysis, fourth ed. Springer, New York, p. 550.

Hinsinger, P., Bell, M.J., Kovar, J.L., White, J., 2021. Rhizosphere processes and root traits determining the acquisition of soil potassium. In: Murell, T.S., Mikkelsen, G.S., Norton, R., Thompson, M.L. (Eds.), Improving Potassium Recommendations for Agricultural Crops. Springer Verlag, New York, pp. 99–117.

ISO, 2018. ISO 23470, Soil quality — Determination of effective cation exchange capacity (CEC) and exchangeable cations using a hexamminecobalt(III)chloride solution.

IUSS Working Group WRB. 2022. World Reference Base for Soil Resources. International soil classification system for naming and creating legends for soil maps. 4th edition. International Union of Soil Sciences (IUSS), Vienna, Austria.

Jouquet, P., Bruand, A., 2023. Bioturbation as a means to circumvent sodium limitation by termites? Suspected processes and ecological consequences. Biol. Fertil. Soils. doi: 10.1007/s00374-023-01752-2.

Jouquet, P., Tessier, D., Lepage, M., 2004. The soil structural stability of termite nests: role of clays in *Macrotermes bellicosus* (Isoptera, Macrotermitinae) mound soils. Eur. J. Soil Biol. 40 (1), 23–29. https://doi.org/10.1016/j.ejsobi.2004.01.006.

Jouquet, P., Bottinelli, N., Shanbhag, R.R., Bourguignon, T., Traoré, S., Abbasi, S.A., 2016. Termites: The Neglected soil engineers of tropical soils. Soil Sci. 181 (3/4), 157–165. https://doi.org/10.1097/SS.0000000000000119.

Julien, J.L., Bourrié, G., Bruand, A., Feller, C., Morlon, P., Van Oort, F., Tessier, D., 2023. Histoire de trois concepts du sol mal maîtrisés: le pH du sol, les cations échangeables et la capacité d'échange cationique. Étude et Gestion Des Sols. 265–281.

Ker, J. C., 1995. Mineralogia, sorção e dessorção de fosfato, magnetização e elementos traços de Latossolos do Brasil. Ph. D. thesis, Universidade de Viçosa, Viçosa-MG, Brasil. 181 p.

LAS, 2023. Laboratoire d'Analyse des Sols INRAE. Catalogue analytique 2023_V1.

Lavelle, P., Spain, A., Fonte, S., Bodano, J.C., Blanchart, E., Galindo, V., Grimaldi, M., Jimenez, J.J., Velasquez, E., Zangerlé, A., 2020. Soil aggregation, ecosystem engineers and the C cycle. Acat Oecologia 105, 103561. https://doi.org/10.1016/j.actao.2020.103561.

Maquere, V., Laclau, J.P., Bernoux, M., Saint-Andre, L., Gonçalvez, L.M., Cerri, C.C., Piccolo, C., Ranger, J., 2008. Influence of land use (savanna, pasture, Eucalyptus plantations) on soil carbon and nitrogen stocks in Brazil. Eur. J. Soil Sci. 59, 863–877. https://doi.org/10.1111/j.1365-2389.2008.01059.x.

Marchi, G., Silva, V.A., Guilherme, L.R.G., Lima, J.M., Nogueira, F.D., Guimarães, P.T.G., 2012. Potassium extractability from soils of Brazilian coffee regions. Biosci. J. 28, 913–919.

Marques, F.A., Calegari, M.R., Vidal-Torrado, P., Buurman, P., 2011. Relationship between soil oxidizable carbon and physical, chemical and mineralogical properties of Umbric Ferralsols. B. Bras. Ci. Solo 35, 25–40. https://doi.org/10.1590/S0100-06832011000100003.

Martin, H.W., Sparks, D.L., 1985. On the behavior of nonexchangeable potassium in soils. Comm. Soil Sci. Plant Anal. 16, 133–162. https://doi.org/10.1080/00103628509367593.

Melo, G.W., Meurer, E.J., Pinto, L.F.S., 2004. Potassium-bearing minerals in two oxisols of Rio Grande do Sul State. Brazil. R. Bras. Ci. Solo 28, 597–603. https://doi.org/10.1590/S0100-06832004000400002.

Meurer, E.J., Anghinoni, I., 1993. Disponibilidade de potássio e sua relação com parâmetros de solo. R. Bras. Ci. Solo 17, 375–382.

Moterle, F.M., Bortoluzzi, E.C., Kamisnki, J., Rheinheimer, D.S., Caner, L., 2019. Does Ferralsol clay mineralogy maintain potassium long-term supply to plants? Rev. Bras. Cienc. Solo 43, e0180166.

Moterle, D.F., Kaminski, J., Rheinheimer, D.S., Caner, L., Bortoluzzi, E.C., 2016. Impact of potassium fertilization and potassium uptake by plants on soil clay mineral assemblage in South Brazil. Plant Soil 406, 157–172. https://doi.org/10.1007/s11104-016-2862-9.

Mujinya, B.B., Mees, F., Erens, H., Dumon, M., Baert, G., Boeckx, P., Ngongo, M., Van Ranst, E., 2013. Geoderma 192, 304–315. https://doi.org/10.1016/j.geoderma.2012.08.010.

Nascimento, D.T.F., Novais, G.T., 2020. Clima do Cerrado: dinâmica atmosférica e características, variabilidades e tipologias climáticas. Élisée, Rev. Geo. UEG – Goiás 9, 2, e922021. https://www.revistadehistoria.ueg.br/index.php/elisee/issue/view/564.

Öborn, I., Andrist-Rangel, Y., Askegaard, M., Grant, C.A., Watson, C.A., Edwards, A.C., 2005. Critical aspects of potassium management in agricultural systems. Soil Use Manag. 21, 102–112. https://doi.org/10.1111/j.1475-2743.2005.tb00414.x.

Oliviera, J.S., Inda, A.V., Barron, V., Torrent, J., Tiecher, T., Camargo, F.A.D., 2020. Soil properties governing phosphorus adsorption in soils of Southern Brazil. Geoderma Reg. 22, e00318.

Pacheco, A.A., Ker, J.C., Schaefer, G.E.G.R., Fontes, M.P.F., Andrade, F.V., Martins, E.S., Oliviera, F.S., 2018. Mineralogy, micromorphology and genesis of soils with varying drainage along a hillslope on granitic rocks of the Atlantic forest biome. Brazil. R. Bras. Ci. Solo 42, e0170291.

Pal, D.K., Srivastava, P., Durge, S.L., Bhattacharyya, T., 2001. Role of weathering of fine-grained micas in potassium management of Indian soils. Appl. Clay Sci. 20, 39–52. https://doi.org/10.1016/S0169-1317(01)00044-8.

Pansu, M., Gautheyrou, J., 2006. Handbook of Soil Analysis. Mineralogical, Organic and Inorganic Methods. Springer-Verlag Berlin Heidelberg, 993 p.

Pédro, G., 1968. Distribution des principaux types d'altération chimique à la surface du globe. Rev. Géogr. Phys. Géol. Dyn. X 457–470.

Poss, R., Fardeau, J.C., Saragoni, H., Quantin, P., 1991. Potassium release and fixation in Ferralsols (Oxisols) from Southern Togo. J. Soil Sci. 42, 649–660. https://doi.org/10.1111/j.1365-2389.1991.tb00111.x.

Qafoku, N.P., Van Ranst, E., Noble, A., Baert, G., 2004. Variable charge soils: their mineralogy, chemistry and management. Adv. Agron. 84, 159–215. https://doi.org/10.1016/S0065-2113(04)84004-5.

Reatto, A., 2009. Nature et propriétés de l'horizon diagnostic de Latosols du Plateau Central brésilien. Thèse Université d'Orléans, p. 195.

Reatto, A., Bruand, A., Silva, E.M., Martins, E.S., Brossard, M., 2007. Hydraulic properties of the diagnostic horizon of Latosols of a regional toposequence across the Brazilian Central Plateau. Geoderma 139, 51–59. https://doi.org/10.1016/j.geoderma.2007.01.003.

Reatto, A., Bruand, A., Martins, E.S., Muller, F., Silva, E.M., Carvalho Jr, O.A., Brossard, M., 2008. Variation of the kaolinite and gibbsite content at regional and local scale in the Latosols of the Brazilian Central Plateau. C.R Geosci. 340, 741–748. https://doi.org/10.1016/j.crte.2008.07.006.

Reatto, A., Bruand, A., Martins, E.S., Muller, F., Silva, E.M., Carvalho Jr, O.A., Brossard, M., Richard, G., 2009a. Development and origin of the microgranular structure in Latosols of the Brazilian Central Plateau: significance of texture, mineralogy and biological activity. Catena 76, 122–134. https://doi.org/10.1016/j.catena.2008.10.003.

Reatto, A., Bruand, A., Silva, E.M., Guégan, R., Cousin, I., Brossard, M., Martins, E.S., 2009b. Shrinkage of microaggregates in Brazilian Latosols during drying: significance of the clay content, mineralogy and hydric stress history. Eur. J. Soil Sci. 60, 1106–1116. https://doi.org/10.1111/j.1365-2389.2009.01189.x.

Reatto, A., Bruand, A., Guilherme, L.R.G., Martins, E.S., Medrado, E., Brossard, M., Muller, F., 2010. Geochemical processes in Latosols on the geomorphic surfaces from Brazilian Central Plateau. 19Th World Congress of Soil Science, Soil Solutions for a Changing World.

Rodrigues Netto, A., 1996. Influência da mineralogia da fração argila sobre propriedades físico-químicas de solos brasileiros. Universidade de Viçosa, Viçosa-MG, Brasil. Ph. D. thesis.

Sardans, J., Peñulas, J., 2015. Potassium: a neglected nutrient in global change. Glob. Ecol. Biogeogr. 24, 261–275. https://doi.org/10.1111/geb.12259.

Schaefer, C.E.G.R., Fabris, J.D., Ker, J.C., 2008. Minerals in the clay fraction of Brazilian latosols (Oxisols): a review. Clay Miner. 43, 1–18. https://doi.org/10.1180/claymin.2008.043.1.11.

Soares, M.R., Alleoni, L.R.F., Vidal-Torrado, P., Cooper, M., 2005. Mineralogy and ion exchange properties of the particle size fractions of some Brazilian soils in tropical humid areas. Geoderma 125, 355–367. https://doi.org/10.1016/j.geoderma.2004.09.008.

Soil Survey Staff, 2022. Keys to Soil Taxonomy. 13th ed. United States Department of Agriculture, Natural Resources Conservation Service, Washington, DC, USA.

Tawornpruek, S., Kheoruenromne, I., Suddhiprakarn, A., Gilkes, R.J., 2006. Properties of red Oxisols on calcareous sedimentary rock in Thailand. Geoderma 136, 477–493. https://doi.org/10.1016/j.geoderma.2006.04.022.

van Wambeke, A., 1992. Soils of the Tropics: Properties and appraisal. McGraw-Hill, London.

Velde, B., Meunier, A., 2008. The Origin of clay minerals in soils and weathered rocks. Springer-Verlag, Berlin Heidelberg, p. 406p.

Volf, M.R., Benites, V.M., Azevedo, A.C., Moraes, M.F., Tiritan, C.S., Rosolen, C.A., 2023. Soil mineralogy and K reserves in soils from the Araguaia River valley, Brazil. Geoderma Regional 33, e00654.